The role of land use on the local climate and air quality during calm inter-monsoon in a tropical city.

OOI, M.C.G., CHAN, A., ASHFOLD, M.J., OOZEER, M.Y., MORRIS, K.I. and KONG, S.S.K.

2019

Geoscience Frontiers 10 (2019) 405–415

HOSTED BY

Contents lists available at ScienceDirect

China University of Geosciences (Beijing)

Geoscience Frontiers

journal homepage: www.elsevier.com/locate/gsf

Research Paper

The role of land use on the local climate and air quality during calm inter-monsoon in a tropical city

M.C.G. Ooi [a,b,*], A. Chan [b], M.J. Ashfold [c], M.Y. Oozeer [b,f], K.I. Morris [d,e], S.S.K. Kong [a]

[a] Department of Atmospheric Science, National Central University, Chung-Li, Chinese Taipei
[b] Department of Civil Engineering, University of Nottingham Malaysia Campus, Malaysia
[c] School of Environmental and Geographical Sciences, University of Nottingham Malaysia Campus, Malaysia
[d] Center of Excellence for Sustainable Innovation and Research Initiative (CESIRI), Port Harcourt, Rivers State, Nigeria
[e] Department of Mechanical Engineering, Ashesi University College, Berekuso, Ghana
[f] Department of Geography and Environmental Management, University of Waterloo, Canada

ARTICLE INFO

Article history:
Received 6 April 2017
Received in revised form
12 December 2017
Accepted 14 April 2018
Available online 9 May 2018

Keywords:
Land use change
Urban
Ground ozone
TVOC
WRF-Chem
Tropics

ABSTRACT

The modification of land use is known to be a major climate change driver to the local warming and air quality in cities. Despite the reduction of NO_x over the years, the Selangor state has captured a higher level of O_3 in year 2011. The measurement result has shown that the surge in O_3 level was attributed to the reduction of NO_x/NMHC ratio. This paper hence attempted to identify the role of land use change from 1999 to 2011 on the ground ozone air quality in the tropical urban conurbation, Greater Kuala Lumpur (GKL), Selangor, Malaysia. With the state-of-the-art chemical weather prediction tool, WRF-Chem, the external synoptic factors and emission inventory were controlled when comparing the chronological land use changes. The results showed that the urban-induced temperature and wind bias in the tropical region has induced stronger wind to disperse the NO_x and carries the TVOC from the suburban to the downwind urban region. The reduction of NO_x/TVOC has gradually shifted towards the optimum O_3 formation regime in 2011. The formation of highly concentrated ozone becomes more sensitive to the increment of TVOC as the NO_x level reduces in the urban. This highlights the essential involvement of TVOC in the ozone formation in lieu of the NO_x reduction in the tropical city, a region with growing emitter of reactive biogenic ozone precursors.

1. Introduction

Urbanization-induced land use change is one of the crucial climate change drivers in expanding cities (Oke, 1973, 1976; Stewart and Oke, 2012). The land use conversion, for urbanization and agriculture, heavily contributes to surface temperature variation (Kalnay and Cai, 2003; Zhang et al., 2011). In urban, the maximization of land use functionality replaces the under-utilized natural surfaces for packed and impervious man-made structures (Oke and Maxwell, 1975; Akbari et al., 2008). Such surfaces absorb and store massive heat during the day (Dimoudi and Nikolopoulou, 2003; Gao and Jia, 2013) and as the height of buildings increases the reradiated heat is trapped within the urban canopy. This thereby increases the ambient temperature and boundary layer height at night (Civerolo et al., 2007; Wang et al., 2007; Li et al., 2013), and reduces the airflow within the urban canopy layer (layer from ground up to average height of the buildings) (Martilli et al., 2002; Thompson et al., 2007; Grossman-Clarke et al., 2008). Foley et al. (2005) emphasized the environmental implication of anthropogenic land use conversion in modern years and described urban heating as “an extreme case of how land use modified regional climate”.

The alteration of physical and thermal properties of land surface has also affected the chemical constituents of the urban atmosphere (Foley et al., 2005; Mahmood et al., 2010; Pielke et al., 2011). Ground ozone (O_3), a component in urban smog, is well related to the aggravation of human respiratory and pulmonary health (Bell et al., 2004; Lacour et al., 2006). The higher nocturnal O_3 concentration in few large urban agglomerations was associated with

* Corresponding author. Department of Civil Engineering, University of Nottingham Malaysia Campus, Malaysia.
E-mail addresses: chelgee.ooi@gmail.com, kebx2oce@nottingham.edu.my (M.C.G. Ooi).
Peer-review under responsibility of China University of Geosciences (Beijing).

https://doi.org/10.1016/j.gsf.2018.04.005

urban-induced warming (Wang et al., 2007; Jiang et al., 2008; Yu et al., 2012). Photochemical O_3 production is limited during the night hence the O_3 level is mainly governed by the chemical loss mechanism of ozone ($NO + O_3 \rightarrow NO_2 + O_2$). In urban, the anthropogenic heat and surface heat retained at night induce atmospheric instability and vertical mixing of the lower atmosphere. This aided the dilution of the major titration component of O_3, nitrogen monoxide (NO) and hence rises the nocturnal O_3 concentration (Ryu et al., 2013a; Li et al., 2014). Ambient humidity was generally known to reduce to O concentration for ozone generation through the wet-scavenging of the O (^{1}D) radical (quenched O (^{1}D)) as O) and inhibition of O_2 photolysis ($O_2 + hv \rightarrow O + O$) through attenuation of sunlight (Ono et al., 2014). The reduction of midday ozone under humid condition was also related to the dry deposition through stomatal conductance (Kavassalis and Murphy, 2017). These also explained the higher ozone level that often observed in the dry urban environment with less vegetation cover (Romero et al., 1999; Civerolo et al., 2000; Jiang et al., 2008). The calm wind condition within the urban region was one of the contributing factors to the accumulation of O_3 precursors and O_3 exceedance (Civerolo et al., 2000; Duenas et al., 2002). Frequently, the pollutant trapped during calm night caused the morning exceedance of pollution level (Wang et al., 2007; Lai and Cheng, 2009). Therefore, the surface heat forcing driven by urban land surface has greatly influenced the flux dynamics of the atmospheric boundary layer and influence the pollutant transportation (Civerolo et al., 2007; Sertel et al., 2009; Zhang et al., 2011).

Regardless of the climatic zone, the nocturnal urban heating rate is found to logarithmically proportionate to the population density due to modification of urban morphology, local wind flow and its energy balances (Oke, 1976; Roth, 2007; Lee et al., 2014; Zhao et al., 2014). Hence, developing countries have expectedly experienced the most rapidly increasing urban heating for the past 40 years (Akbari et al., 1992; Kataoka et al., 2009). The United Nations (UN) census statistics reported that the urban population in Malaysia has exceeded 60% of the national population and the growth rate stayed ahead of the average condition of Southeast Asia (SEA) and Asia countries (United Nations, 2014). Greater Kuala Lumpur (GKL), also known as Klang Valley is the most urbanized conurbation of Malaysia (Department of Statistics, 2011). The conurbation covers the country's capital, Federal Territory of Kuala Lumpur and Putrajaya, alongside with its surrounding agglomerated cities within the state of Selangor as shown in Fig. 1. The region falls under the wet and hot tropical climate. Studies in Malaysia have shown that the daily maximum of ozone level approximates 50 ± 20 ppbv (Banan et al., 2013). The highest ozone concentration and prolonged exceedance (>100 ppbv; Department of Environment, 2013) were often recorded at stations located near the residential region with close proximity to the highly developed urban cluster or industrial area (Latif et al., 2012; Ahamad et al., 2014). Most previous work on effect of urbanization on local climate and air quality were conducted through analytical work of air quality recorded from ground measurement stations. Although it provided a valuable local information, it has generic difficulty to scrutinize the spatio-temporal influence of urbanization through land use change. The ozone formation in the region is correlated with meteorological condition and primary pollutants while the interactive role of both

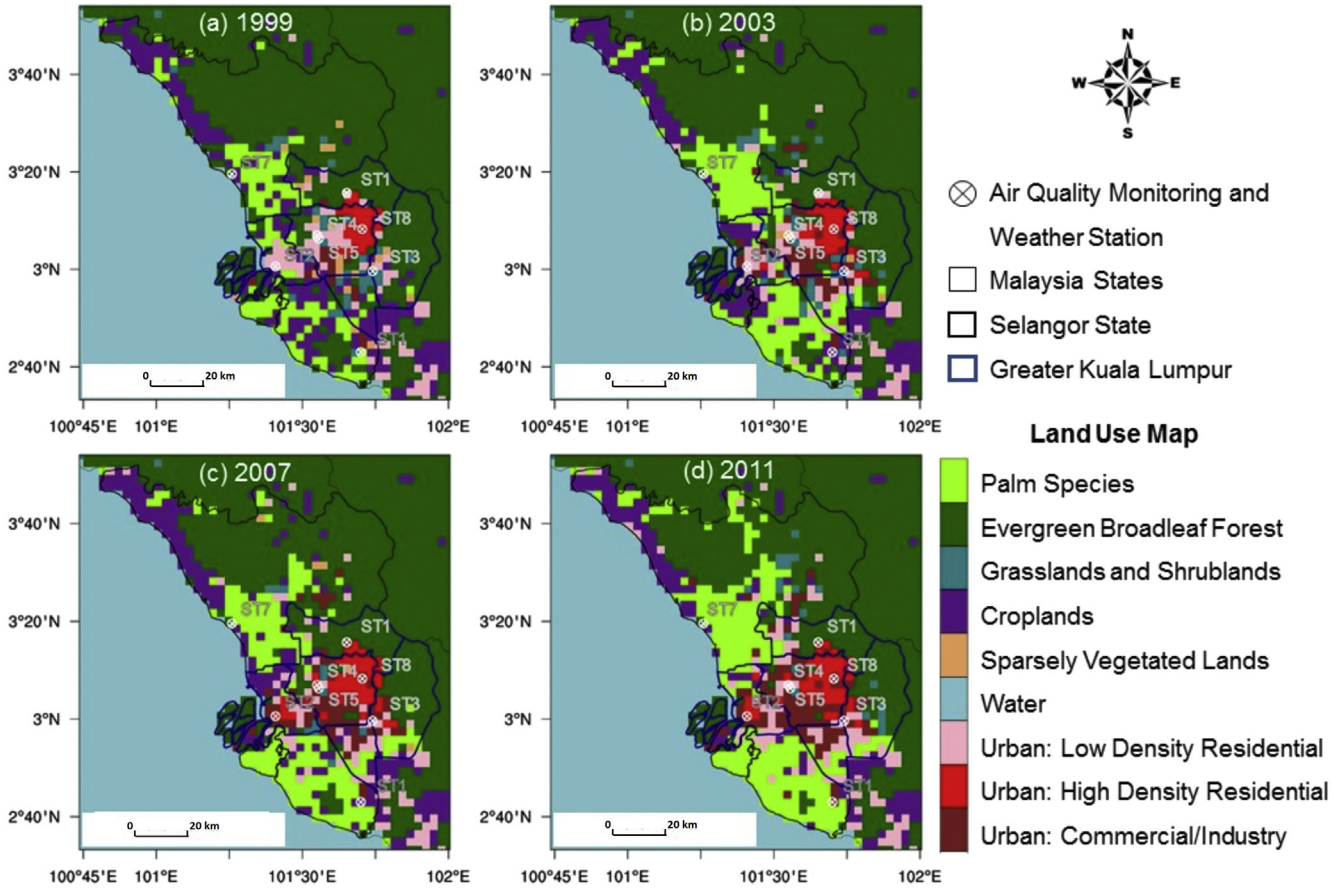

Figure 1. Location of ground weather and air quality stations are marked with black markers, refer to Table 1 for the description of each weather station. Updated LU map in year (a) 1999, (b) 2003, (c) 2007 and (d) 2011.

factors in ozone formation is thus far neglected (Ahamad et al., 2014; Tan et al., 2014).

Seeing that the ozone formation is subjected to the concurrent factors involving the emission from urban sources, the current effort to identify the effect of land use change urbanization in the region on the air quality condition is still not well established. Therefore, in Section 2, the background pollutant level study during the period of study is analysed to comprehend yearly and hourly change of the ground ozone level as well as its ozone precursors. In Section 3, numerical modelling tool is deployed to account for the isolate the effect of synoptic climatic forcing and background atmospheric composition from the ozone formation process. The applicability of model is first examined against the near-surface and vertical meteorological parameters as well as the air pollutants in Section 4. It is then configured to scrutinize the effect of land use change on the variation of atmospheric pollutant, especially ground ozone in Section 5. From which, the urban-induced changes of local weather and circulation pattern are subsequently studied to comprehend the contributing extend of the featured urban environment to the air quality issue.

2. Background weather and air quality

The study focused on the effect of urban-induced local climate change and avoided the period of strong synoptic forcing. The calm inter-monsoon period, April 2003 was hence studied (Jauregui et al., 1992; Tangang, 2001; Santamouris, 2015). In this period, the GKL region was dominated by weak winds with less defined direction. Such weather condition was more conducive to the accumulation of pollutant with the higher atmospheric ground O_3 amount measured (Latif et al., 2012). On average, April experienced higher daytime temperature above 30 °C and relative humidity above 60%. Convective raining with thunderstorm occurred during the late afternoon from 1400 MYT to 2000 MYT (Sow et al., 2011; Bhatt et al., 2016).

The chronological pollutant measurement data in April were studied at a consistent four-year interval at 1999, 2003, 2007 and 2011. The updated land use maps for Selangor state from 1999 and 2011 at every 4-year intervals were illustrated in Fig. 1. The urban land use in Selangor state grows from 14% to 29% of total land use and it mainly replaced the evergreen broadleaf forest which decreased from 48% to 35% from 1999 to 2011. While the urbanization has concentrated in the GKL agglomeration with 22.6% increment of urban land use. The urban land use composition (including LDR, HDR, COM) increased by a total of 9.1%, around 820 km^2 from 1999 to 2011. Fig. 1 also marked the location of eight air quality monitoring stations with details given in Table 1. The numbers of functioning stations for each measured pollutant in the studied years are tabulated in Table 2.

Table 1
Information on weather station for meteorological verification and air quality with latitude (Lat) and longitude (Long) location and corresponding land use for each ground observation station. The urban land use has three urbanization levels: low-density residential (LDR), high-density residential (HDR) and commercial/industrial region (COM).

Station code	Station name	Lat (°N)	Long (°E)	Operator	Land use
ST1	Gombak	3.262	101.652	JAS	Urban (COM)
ST2	Klang	3.010	101.408	JAS	Urban (LDR)
ST3	Kajang	2.994	101.740	JAS	Urban (HDR)[a]
ST4	Shah Alam	3.105	101.556	JAS	Urban (COM)
ST5	Subang	3.117	101.550	MMD	Urban (COM)[a]
ST6	Sepang	2.717	101.700	MMD	Croplands adjacent to Urban (COM)
ST7	Kuala Selangor	3.327	101.259	JAS	Grasslands and shrubs
ST8	KL	3.138	101.705	JAS	Urban (HDR)

[a] The station is in urban land use that is surrounded by grasslands and shrubs.

Table 2
Number of functioning air quality monitoring stations in April during study years.

Year	Air pollutants			
	Hourly/8-hourly O_3	NO_2	NO	NMHC
1999	7	7	7	5
2003	8	8	8	7
2007	8	8	8	6
2011	6	6	6	0

The concentration of photochemical pollutant, O_3 was at its maximum level during the day (hourly ozone: 1400–1500 MYT) and quickly depleted in the evening as shown in Fig. 2a. Dissimilar with the ozone concentration which peaked during the day, NO and NMHC recorded a sharp morning peak (0800–0900 MYT) and an evening peak after 2200 MYT in Fig. 2d and h. The double peaks were ubiquitously observed in other cities (Pudasainee et al., 2006; Han et al., 2011; Ryu et al., 2013a,b). The concurrent peaks indicated the emissions source originated from incomplete combustion cycle of engines during working rush hours of the city. The oxidized products of the hydrocarbons, HO_2 and RO_2 are not readily recorded through the measurement, but they contribute immensely as a strong driving agent for the NO to NO_2 oxidizing process. In Fig. 2e, the NO_2 therefore surged an hour later and supplied activated oxygen atom as raw material for O_3 formation. The NO_x level was lower during the day time due to the reactive O_3 photochemical reaction and also the noontime heat convection which enhanced dispersion (Ooka et al., 2011; Ryu et al., 2013a,b). The absence of solar radiation inhibited the photolysis reaction and hence the NO_2 levels increased during the evening. The concentrated amount of NO_2 converted back into the initial NO form and around at 0000 MYT.

The daytime peak O_3 concentration has recorded the lowest (35 ± 16 ppbv) in 1999 and highest (47 ± 13 ppbv) in 2011 among the years investigated in Fig. 2a. The stronger wind flow in 1999 during the day (see Fig. 2c) correlated well with the lower concentration NO_2 and NMHC, which are the main O_3 precursors. Conversely, year 2003 with relatively low wind speed corresponded to the higher pollutant concentration of NO, NO_2 and NMHC. Despite the surge of these ozone precursors, the level of O_3 was not exceptionally higher in 2003 compared to the remaining years. Such phenomenon also could not be related in 2011 with a moderate wind speed.

The morning rush-hour spike of NO is most apparent in 2003 with a notable rise in nocturnal concentration. The NO level shows a clear reduction (around 30 ppbv) in 2007 and dropped by another 10 ppbv in 2011. However, it was observed that the reduction of the anthropogenic pollutant did not significantly reduce the O_3 level, in turn, it increased greatly in year 2011 with lowest NO. In Fig. 2f, the higher value of NO_2/NO was observed in 2007 and 2011 during the day generated a greater level of oxidant and hence the growth of O_3 level. Inversely, it also applied to the lowest daytime O_3 level in 1999. Therefore, despite the highest value of individual NO and NO_2 species recorded in 2003, the ozone level was not exceptionally higher due to the moderate NO_2/NO ratio. The NO_2/NO ratio indicated the photolysis potential of NO_x to produce oxygen atom to fuel O_3 generation. However, this ratio has ideally assumed the loss and generation of O_3 depended on the conversion of NO to NO_2 in the null cycle of NO_2, NO and O_3 reaction (Han et al., 2011). It did not account for the entire complexity of the photochemistry reaction in real time. For instances, O_3 did not involve in the removal of NO_x through deposition, production of NO_2 from NO and O_2 as well as

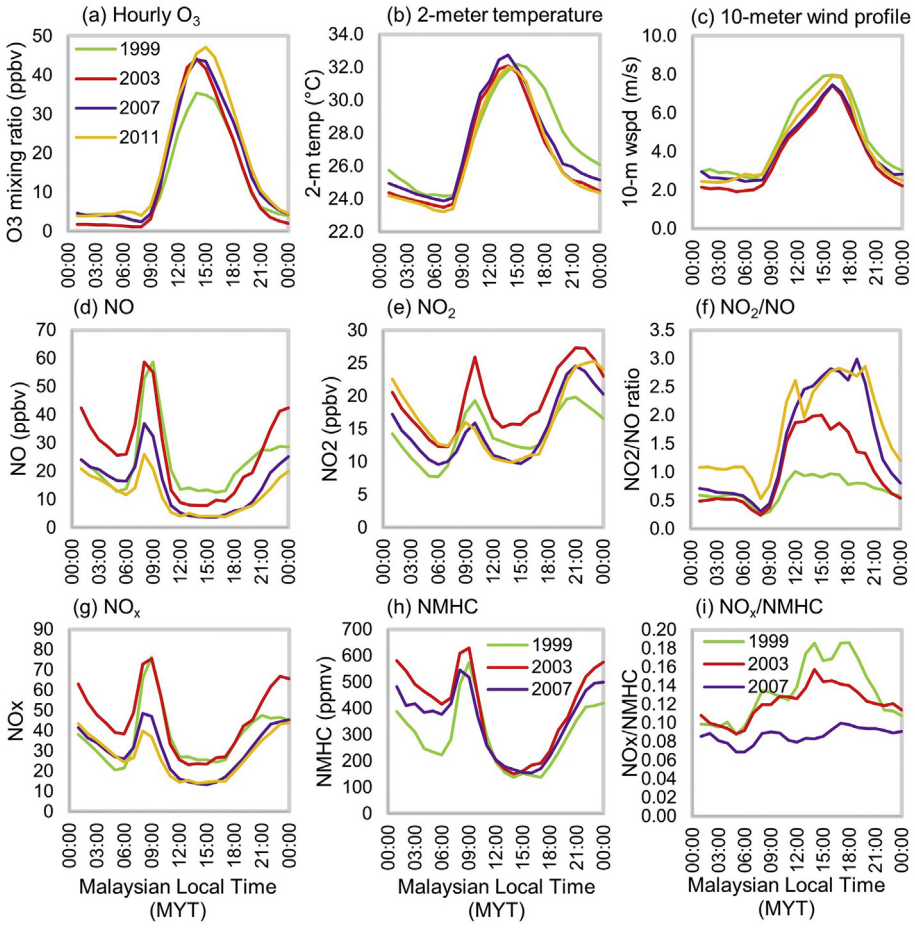

Figure 2. Diurnal hourly averaged (a) O_3, (b) 2-m temperature, (c) 10-m wind speed, (d) NO, (e) NO_2, (f) NO_2/NO, (g) NO_x, (h) NMHC, (i) NO_x/NMHC in April of 1999, 2003, 2007, 2011.

conversion between NO and NO_2 by other peroxyl radicals (Clappa and Jenkin, 2001; Pusede et al., 2015).

The ratio of NO_x (NO + NO_2) to NMHC was then investigated to identify the sensitivity regime of the formation of O_3 (Sillman, 1999) and to account the processes overlooked by the previous indicator. It was known that O_3 concentration increases linearly with NO_x and NMHC when they present at low concentration respectively. However, continual increment of individual species limits the others and reduces the ozone production. Hence, the local maxima of ozone occurred within an optimum ratio of NO_x and NMHC. From which, the region above the optima inclines to the NMHC-sensitive regime and the below inclines the NO_x-sensitive regime. The measurement of NMHC was discontinued after 2007, hence, the analysis is conducted up to 2007 as shown in Table 2. The comparison focused on the period of 1100–1900 MYT with the highest O_3 formation rate and NO_2/NO ratio. The level of O_3 was shown in transitions of colour in the NO_x versus NMHC plot in Fig. 3. The best-fitted line of NO_x/NMHC showed the general distribution slope of the entire year. It was found that the daytime NO_x/NHMC ratio (1100–1900 MYT) of the measured data decreased

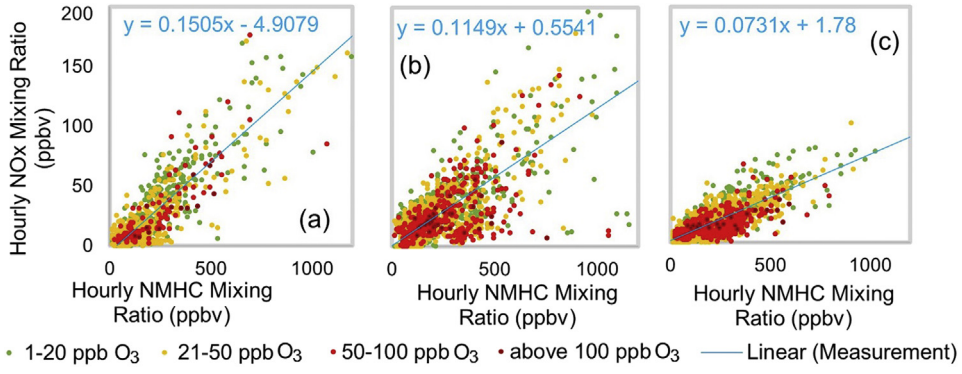

Figure 3. Concentration distribution of O_3 in the NMHC and NO_x xy-plot from 1100 MYT to 1900 MYT in April (a) 1999, (b) 2003, (c) 2007.

from 0.1505 (1999), 0.1149 (2003) to 0.073 (2007). It resonated with above increment of ozone from 1999 to 2007. Such circumstance suggested that the reduction of NO_x/NMHC falls, if not, was approaching the optimum O_3 formation regime. It resonated with the highest O_3 recorded in 2011 with the continuous reduction of NO_x from 2007, as shown in Fig. 2a and g. Hence, the O_3 level was likely to increase due to the reduction of NO_x. Another plausible projection for the level of O_3 was the increment of NMHC in the region. This was particularly critical seeing the rapid expansion of palm plantation (around 650 km^2) as seen Fig. 1. The maturity of the plantation is likely to emit a large amount of isoprene, a highly reactive O_3 precursor (Silva et al., 2016).

The meteorological factors, particularly temperature is a common indicator of urban-induced heat. However, the measurement result is unable to isolate the urbanization effect in the measurement study since its signal might be mixed with the variation of climatic forcing and green-house effect. The numerical model was subsequently run to focus on the effect of land use change on the atmospheric composition through the enhanced surface forcing of the urbanization effect.

3. Model physics and experiment design

Weather Research and Forecast software with ARW dynamical core (WRF-ARW) in combination with the online chemistry model, typically known as WRF-Chem, was deployed to study the implication of urban land use change over the years (1999, 2003, 2007 to 2011) on the regional air composition. The cases were named as LU1999, LU2003, LU2007 and LU2011 respectively. The simulations were run with the same initial and lateral boundary weather condition and emission inventories for the same period to effectively control the influence of synoptic weather variation or atmospheric chemistry composition on the urbanization effect. The simulation period started from 1st April 2003 and lasts for 9 days and the first day served as the spin-up period for steady throughout.

The parent domain (d01) covering entire Malaysia with 27 km grid size was nested to 9 km covering the Malay Peninsula and finally the third domain (d03) with 3 km resolution to cover the west coast and Selangor state where GKL is located. The domain configuration was shown in Fig. 4. To capture the rapid near-surface atmospheric variability especially for the heterogeneous urban environment, the vertical resolution for the lowest 1 km is covered with 15 full sigma vertical levels, adding into the total of 37 levels from the surface up to the model top at 50 hPa. The updated land use for Selangor state (Fig. 1) was used as the input land use map while single-layer urban canopy model was adopted with the local calibrated urban parameters (Morris, 2016). Mellor-Yamada-Janjić (MYJ) boundary layer scheme was used along with Eta MM5 surface layer scheme with modified MZT roughness length to parameterize the vertical diffusion and turbulence within the boundary and surface layer (Janjic, 2001; Chen and Zhang, 2009). RADM2 was used as gas chemistry packages (Stockwell et al., 1990). MADE/SORGAM was chosen as aerosol size distribution and chemistry packages to include the anthropogenic emissions. MADE was chosen for usage due to its reasonable particle size sorting scheme and flexibility in including additional schemes. SORGAM is able to

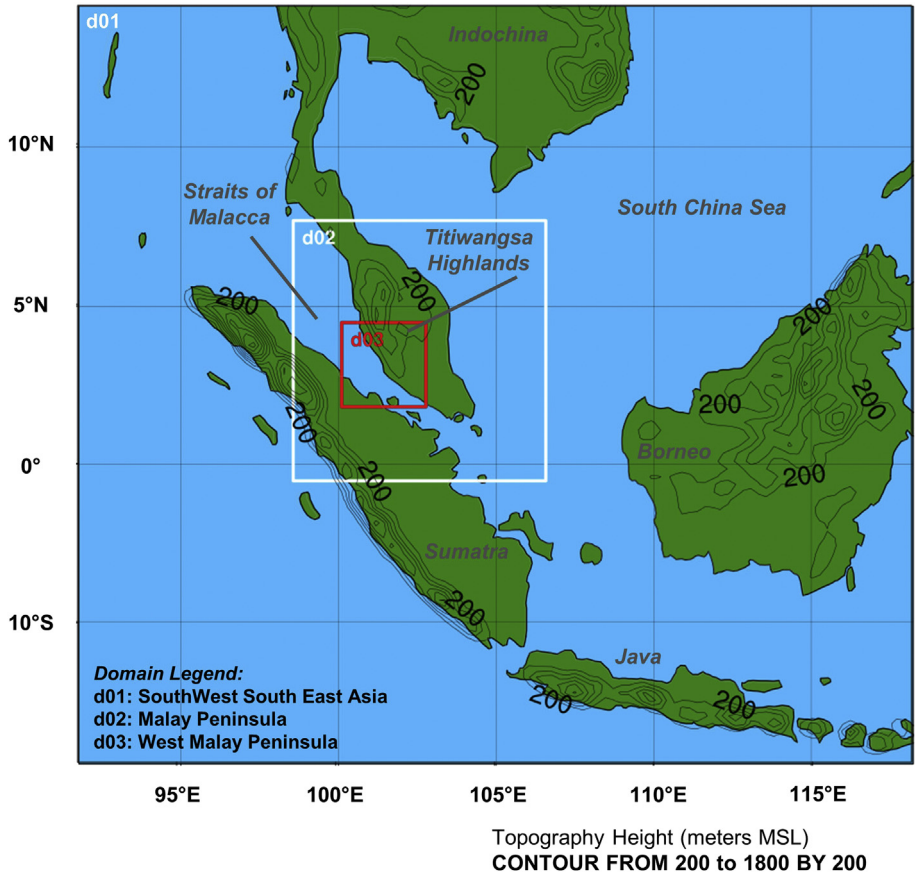

Figure 4. Location map with terrain height information and domain settings of GKL for WRF simulation; d is denoted as domain with the following numbering indicates the number of domain.

Table 3
Model settings and physics options.

Parameters	Value/Option	Parameters	Value/Option
Simulation period	10 days for 2003 (1st April 0800 MYT – 10th April 0800 MYT)	Cumulus scheme	Betts-Miller-Janjić (enabled for d01 and d02)
Analysed period (One-day spin up)	9 days for 2003 (2nd April 0800 MYT – 10th April 0800 MYT)	Lateral boundary data	ERA-interim 6-hourly reanalysis data (Dee et al., 2011)
Domain setting	1st (d01): 27 km (110 × 100) The entire Malaysia including Borneo 2nd (d02): 9 km (100 × 103) Malay Peninsula 3rd (d03): 3 km (100 × 100) West Malay Peninsula	Anthropogenic emission inventories	REanalysis of TROpospheric (RETRO) (Schultz et al., 2007) Emission Database for Global Atmospheric Research (EDGAR) version 4.2
Vertical levels (in eta levels)	37 vertical eta levels. 15 level for bottom 12 km	Chemical boundary data	MOZART-4 (Emmons et al., 2010)
Land surface model (LSM)	Noah LSM coupled with single-layer urban canopy model	Biogenic emission inventory	MEGAN Community Data Portal (CDP) (Guenther et al., 2006)
Planetary boundary layer (PBL) and surface layer scheme	MYJ PBL scheme and Eta MM5 surface layer	Gas chemistry mechanism	RADM2
Radiation scheme (long wave and short wave)	RRTMG	Aerosol size distribution and chemistry mechanism	MADE/SORGAM
Microphysics scheme	Purdue Lin single moment	Biogenic gas chemistry	Online MEGAN

predict the POA (Primary Organic Aerosols) at comparably low computational cost (Ahmadov et al., 2012; Athanasopoulou et al., 2013). Other physics settings and initial and boundary data used were given in Table 3.

4. Model evaluations

With the available data from the 8 ground measurement stations in Table 1, the model was verified its performance to simulate the near-surface weather parameters and atmospheric chemical composition. The model is tested with the four statistical error indices to reflect the conformity of modelled data (Emery et al., 2001; Willmott and Matsuura, 2005; Yu et al., 2006). Mean Absolute Error (MAE) shows the average departure of simulated value from actual result while Root Mean Square Error (RMSE) emphasizes the impact of larger error that runs away from the observation. Both indicators give positive value and the larger value implies large error departure from measured data. The asymmetrical of the result is accounted with Fractional Averaged Error (FAE) by referencing it to the average of both datasets. Seeing that the value range (in fractions) of the latter might be confused with conventional representation, Normalized Mean Absolute Error (NMAE) is therefore introduced to represent the absolute error factor of the mean observation value.

The verification through statistical errors in Table 4 recorded error magnitude for 2-m temperature around 3.3 °C RMSE, 2-m relative humidity around 11.2% RMSE and 10-m wind speed around 3.39 ms^{-1}. Compare to the previous WRF work done, the integration of chemical module creates higher uncertainty to the ground parameters (Ooi et al., 2017). The radiosonde sounding station (ST6) supplies verification data for the vertical boundary weather profile at morning and evening transitional period of 0800–2000 MYT (University of Wyoming, updated daily). The model generally predicted a good agreement of the potential temperature, mixing ratio and wind speed on the vertical scale. The air pollutant concentrations of O_3, NO_x and TVOC were verified on the hourly basis against the measured data. The modelled pollutant level reproduced the diurnal trend and underestimated the NO_x and TVOC concentration as shown in Fig. 5b and c. Owing to the model chemical mechanism used for photochemical aerosols, the modelled TVOC did not account for all the hydrocarbons in the measured NMHC. The limited measurement result explains the large gap in the comparison. Underestimation of these local surface sources, especially NO_x is closely related to the quality of the emission inventory (Tie et al., 2010; Fallmann et al., 2016). The available emission inventories used for the anthropogenic and biogenic emissions are on a global scale, with the resolution of 0.5° (~55 km) monthly and 0.1° (~11 km) yearly data (Schultz et al., 2007; Zhang et al., 2009). The coarse resolution is relatively homogenous considering the model resolution of 3 km and it has surpassed the ability of the model down-scaling. The model overestimated the hourly ground O_3 with an overall RMSE 18 ppbv as tabulated in Table 4. Compared to the emission inventory resolution, the accuracy of modelled O_3 level depended more on the WRF grid resolution, which involved the meteorological forcing from radiation and local wind field (Tie et al., 2010). However, the higher O_3 level remained affected by the underestimated NO_x concentration through reduced titration processes. The modelled pollutants, at this point, was valid to serve as a control case study by comparing the effect of urbanization. However, the quantitative investigation

Table 4
The meteorological model performance of WRF-Chem evaluated through error indices.

Near-surface parameters	2-m temperature (°C)	2-m relative humidity (%)	10-m wind speed (ms^{-1})
Average OBS	26.12	68.0	3.91
MAE	2.02	8.50	2.49
RMSE	3.27	11.24	3.39
FAE[a]	0.075	0.116	0.811
NMAE[a]	0.077	0.125	0.638
Vertical parameters	**Potential temperature (K)**	**Mixing ratio (kg/kg)**	**Wind speed (ms^{-1})**
MAE	0.58	0.70	0.70
RMSE	0.67	1.01	0.84
FAE[a]	0.002	0.054	0.179

[a] FAE and NMAE are dimensionless.

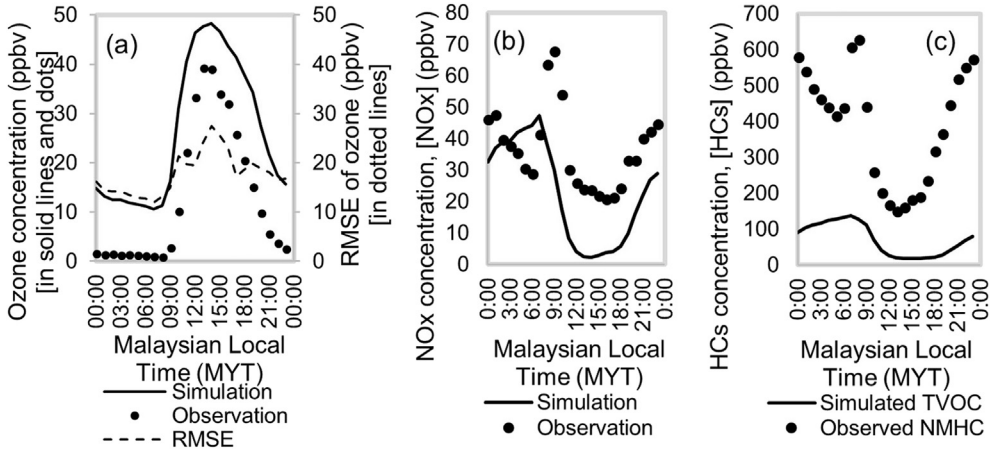

Figure 5. Comparison of hourly-averaged (a) O_3, (b) NO_x, (c) TVOC concentration profile of modelled data to measured data in April 2003.

on the actual amount of pollutant produced could be done, only if the high-quality emission inventory of associated resolution was developed or made available.

5. Effect of urbanization on local climate and air quality

During the day, the urban cooling effect was observed, and the cold bias increased steadily over the years from −0.1 °C (LU2003-LU1999) to −0.2 °C (LU2011−LU1999) around 1000−1200 MYT. This was attributed to the increment of packed urban lands which heat exchanges between the urban canopy and the atmospheric layer above inefficient. The phenomenon known as the cool island effect is commonly detected in the tropical region due to the tall vegetation with greater heat retention capability (Jauregui et al., 1992; Li et al., 2013; Zhao et al., 2014). The cool island effect exerted a high-pressure region which suppresses the vertical mixing and local wind flow in the region. The stronger cooling effect in LU2011 has suppressed and delayed the vertical updraft of the heated air in the GKL region around 1100 MYT. Apart from that, Fig. 6c also showed that ground wind speed is greatly weakened around 1000-1200 MYT when the sea breeze propagated into the region (change of ground wind direction). It is attributed to the urban land use with a larger roughness that slowed down the wind speed entering the urban region (Thompson et al., 2007; Zhong and Yang, 2015). After the sea breeze passage pushed into the urban, the rising warm air near the urban has strengthened the inflow of the sea breeze into the around 1300 MYT. This has subsequently caused the vertical updraft (positive wind speed seen in Fig. 6b) to intensify around 1300−1400 MYT when the cooling effect weakened. Such effect of enhancing wind speed near the urban core is often observed at coastal cities located near to elevated highlands (Freitas et al., 2011; Ryu et al., 2013a,b).

The stronger wind has greatly affected the atmospheric chemical composition in the urban. The NO_x emission with the peak recorded during the morning was dispersed by the strong winds over the years as illustrated in Fig. 6d. Same applied for the TVOC in Fig. 6e but the TVOC level in LU2011 has increased slightly than LU2007, around 7 ppbv. It was observed that O_3 varies the most during the day (1000−1600 MYT) over the year. The O_3 level (Fig. 6a) dropped and the difference has reduced from 4 ppbv (LU2003 - LU1999) to 0.6 ppbv (LU2007−LU2003). In 2011, the O_3 concentration has increased by 3 ppbv compared to LU2007. However, it was still lower than the level of LU1999 from 1300−1600 MYT. Several joint factors were found to contribute to the concentration variations. The relative reduction rate of NO_x and TVOC has increased the NO_x/TVOC ratio in LU2003 and reduces in LU2007 and LU2011. The ozone level in the urban became more limited by the NO_x due to the increased amount of TVOC. The daytime NO_x/TVOC ratio (1100−1900 MYT) decreased over the years from 0.24 to 0.16.

The pollutant distribution for the entire Selangor region, which included the suburban peripheries of GKL region as investigated. In Fig. 6g, O_3 level in Selangor was higher by approximately 3 ppbv compared to GKL. The TVOC level in Selangor (Fig. 6h) was also much higher in Selangor region and agrees with the higher TVOC under stronger wind condition. The rising trend of TVOC was noticeable in the measured data as discussed above. The GKL region is identified as the land-side coastal tropical precipitation regime that features great influence of land-sea breezes (Kikuchi and Wang, 2008) which determines the diurnal local atmospheric chemistry (Wakamatsu et al., 1999). The increment of the TVOC was postulated to be a directional advection following the inflows of strong wind in Fig. 7. Larger O_3 concentration was generally observed while comparing the suburban region to the urbanised region that is NO_x-saturated (Sillman, 1999). A similar decreasing trend of NO_x/TVOC in Selangor was illustrated in Fig. 6i. The O_3 level in LU2011 has even exceeded that of LU1999 in Selangor region when the daytime NO_x/TVOC ratio dropped from 0.15 to 0.09. This indicated that the reduction of NO_x and increasing TVOC has approached the optimized fraction for O_3 production. The ground ozone in the model agreed well with the observation and showed an increasing trend dependent on the reducing NMHC/NO_x ratio.

During the night, the temperature increased with the growing urban land use from LU1999 to LU2011, around doubled from 0.16 °C to 0.38 °C (comparing GKL and Selangor). The vertical wind speed also increased over the years as agreed with the growing boundary layer height. The concentration of NO_x has reduced following the greater mixing at night and thus reduced the nighttime titration effect. The spatial distribution of ozone at 1000 MYT has clearly shown a great contrast between the urbanised region with its surroundings in Fig. 7i–l. The ozone has increased by less than 1 ppbv in LU2011, however, the reduction of ozone was not as apparent compared to the day.

The urban land use has modified the meteorological condition in the GKL and Selangor regions differently during day and night. However, both period (day/night) was related to the increase wind

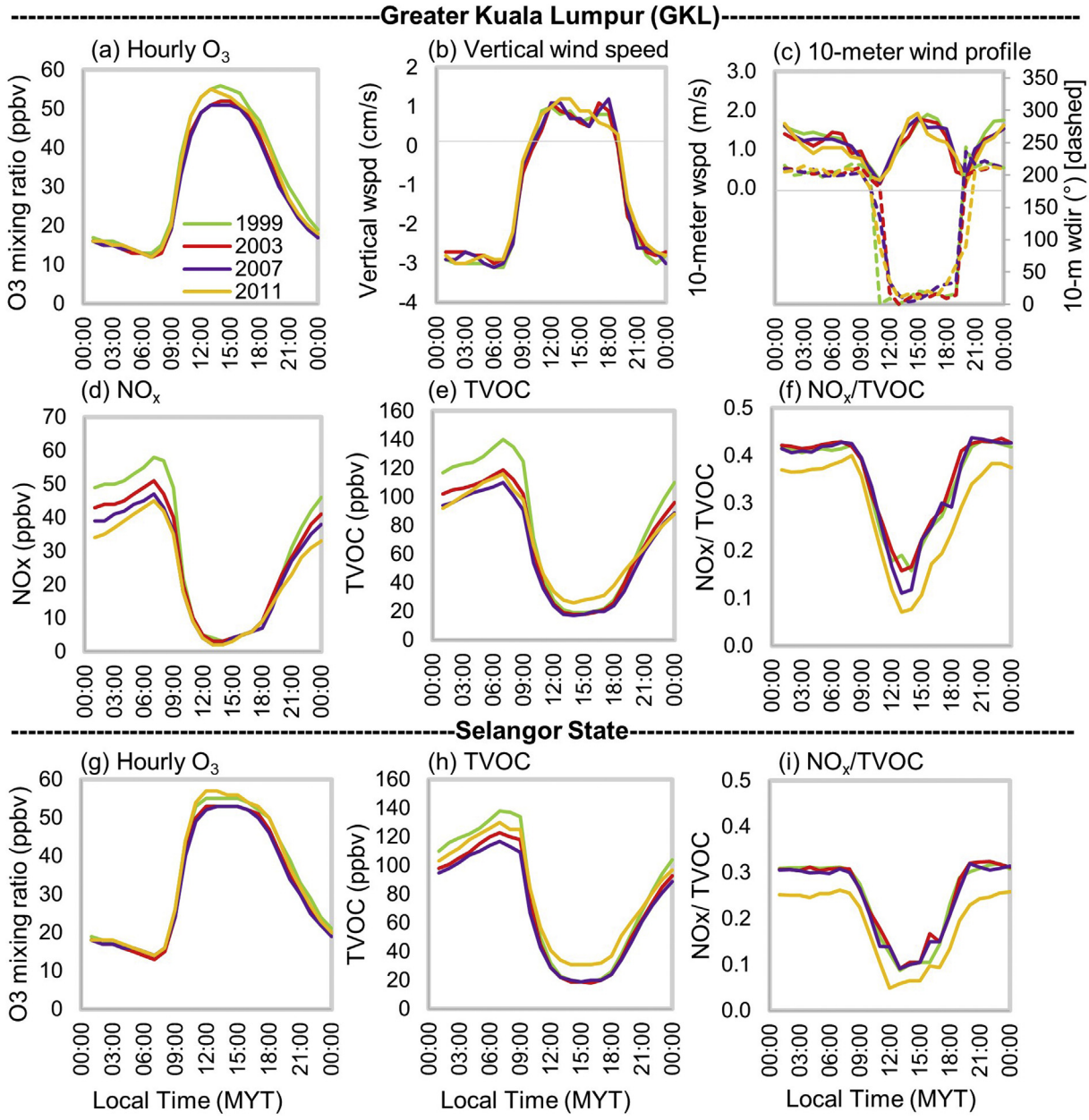

Figure 6. Hourly averaged profile of (a) hourly O_3, (b) vertical wind speed, (c) 10-m wind profile, (d) NO_x, (e) TVOC, (f) NO_x/TVOC for GKL region and (g) O_3, (h) TVOC, (i) NO_x/TVOC for Selangor state for LU1999, LU2003, LU2007 and LU2011.

speed due to temperature change (reduce/increase). Dilution of both NO_x and TVOC levels have contributed to the reduction of O_3 in the initial period. However, in 2011, the NO_x did not reduce further while TVOC has started to increase owing to the inflow from the suburban (industrial) region. The NO_x/TVOC hence gradually approached the optimum ratio for O_3 formation and the O_3 started to increase. Both simulation and measured data observed the similar trends. The modelling has shown that biogenic emission (isoprene) made up of around 20% of the TVOC. The frequency of the 2011 cases is projected to increase owing to the growing popularity of the lucrative plantation (palm species) in the region which emit a high amount of reactive biogenic VOC.

The daytime response of atmospheric pollutant composition due to climatic forcing can reduce the forming potential of ozone. However, the current resolution of chemical boundary data was unable to be captured in the land-sea mask in this study. To tackle the quality of the emission inventory data, approaches were proposed to build emission inventory that produced reasonably accurate the local emission map from the limited measurement information (Streets et al., 2003; Zhang et al., 2009; Wang et al., 2010). With the referenced methodology, a basic inventory could be developed to overcome the incompetency resolution of global emission inventory to apply in the case study region. The locally calibrated inventory database was able to improve the accuracies of anthropogenic emission, which highly dependent on the local anthropogenic activities (Tie et al., 2010; Fallmann et al., 2016). This could subsequently improve the accuracy of the model to estimate the atmospheric composition.

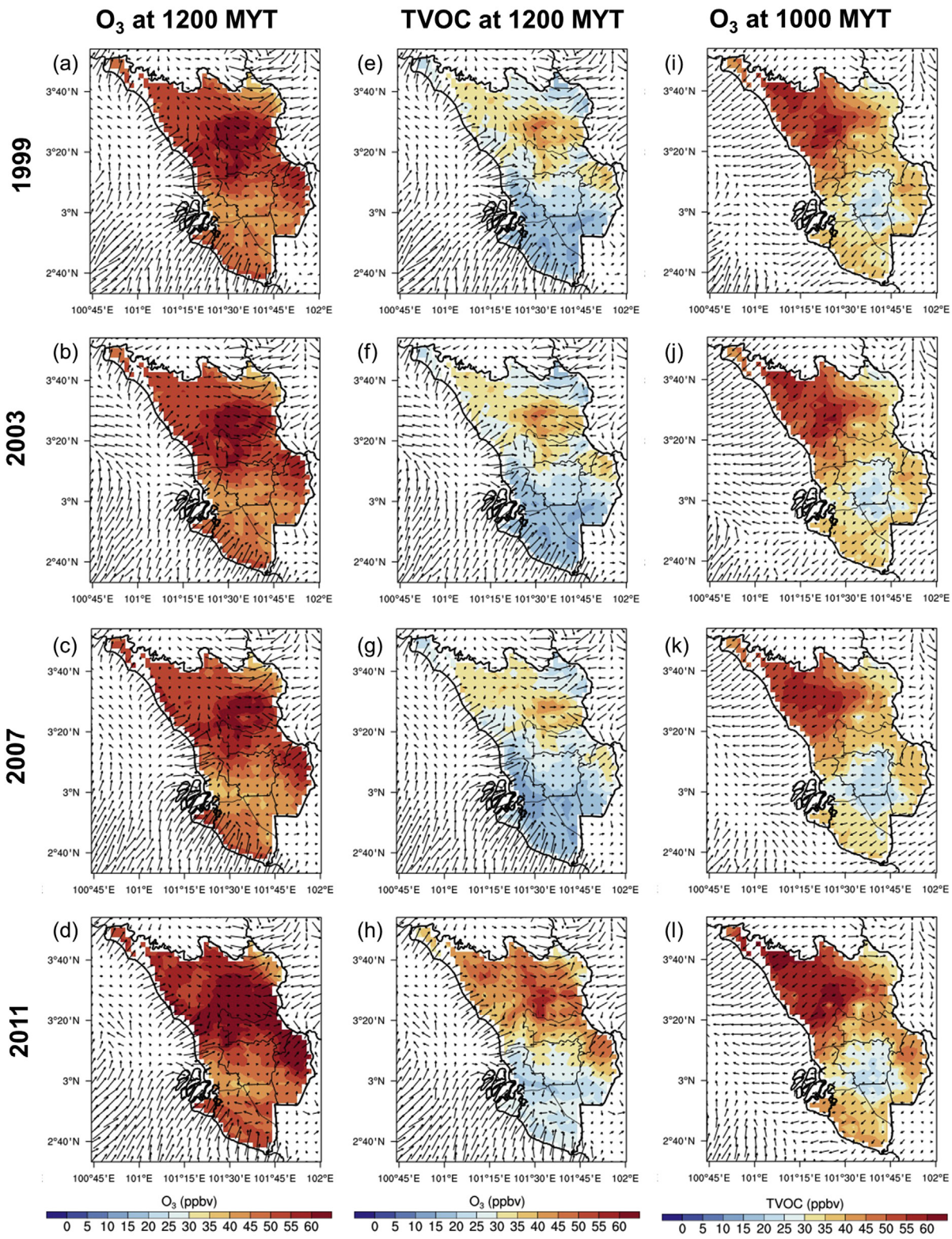

Figure 7. 10-m wind speed and (a–d, i–l) O_3, (e–h) TVOC spatial profile for (a, e, i) LU1999, (b, f, j) LU2003, (c, g, k) LU2007, (d, h, l) LU2011 at (a–h) 1200 MYT and (i–l) 1000 MYT.

6. Conclusions

In this context, the role of urban land use change is discussed as the driver of the climate change and its associated modification of air quality in the tropical urban conurbation, GKL, Selangor, Malaysia. The GKL region has experienced a total expansion of 1400 km^2 of urban land use and 900 km^2 oil palm plantation over a decade time (1999–2011). The pollutant concentration measured that the level of NO_x reduces through the years with occasional surge due to the reduced wind speed as seen in year 2003. The 2-m temperature and

O_3 do not show a clear variation and increment through the years in the GKL region. Nevertheless, the measured ozone was positively correlated with reduced wind speed and increased NO_2/NO ratio under the region with increasing ozone formation sensitivity to NO_x. It is predominantly caused by the growth of NMHC in the region. Therefore, urbanization with surges of NMHC levels was able to stimulate increasing O_3 level in the coming years.

Numerical chemical weather prediction tool, WRF-Chem was deployed to scrutinize the effect of urban land use change on local climate and its climatic forcing on the air quality in the region. The control study focused on the modification of local climate through chronological urban land use change. The GKL region experienced reduced heat and increased physical roughness length concurrently due to urbanization in the morning hours. Transitioning into the afternoon, the increased temperature and wind speed over the region has dispersed the NO_x concentration in the GKL are which reduces the daytime O_3. However, the strong upwind flow has carried TVOC into the urban and increased the O_3 level in the episodic LU2011. The nighttime ozone reduction corresponded well to the urban warming effect that enhanced the local wind circulation and mixing for pollutant dispersion. The overall land use change from 1999 to 2011 showed that the gradual expansion of urban land use increased the ground ozone concentration during the day. It also agrees with the analysis from the measuring data that the ozone formation in urban gradually shifts to the high O_3 forming potential regime. This highlights the essential role of the TVOC emission on the ground ozone formation in the tropical urban compared to the effect of urbanization in terms of urban-induced climatic change.

Despite the essential role in ozone formation, the ground measurement of NMHC was discontinued in all weather stations in Malaysia and prevent further research possibilities. Moreover, the discrimination of the model result has suggested that the urban study required correspondingly high-resolution chemical boundary condition before the output result of chemical constituents was deemed sensible. It was proposed that future research ventures into the selection of suitable emission inventory, if not, the building of inventory for the region. Such research effort was beneficial to stimulate and attracted more research interest in the SEA region. Notwithstanding its limitations, this study has offered some insight into the effect of urbanization in the SEA tropical region that is experiencing a rapid change of land use.

Acknowledgments

The authors would like to thank the Ministry of Science Technology and Innovation (MOSTI) of Malaysia for providing financial support for this research work. This work is partly sponsored under contract No. 06-02-12-SF0346. The authors would also like to thank University of Nottingham Malaysia Campus for awarding a research scholarship. We are also grateful for access to the University of Nottingham High Performance Computing Facility.

References

Ahamad, F., Latif, M.T., Tang, R., Juneng, L., Dominick, D., Juahir, H., 2014. Variation of surface ozone exceedance around Klang Valley, Malaysia. Atmospheric Research 139, 116–127. https://doi.org/10.1016/j.atmosres.2014.01.003.

Ahmadov, R., McKeen, S.A., Robinson, A.L., Bahreini, R., Middlebrook, A.M., deGouw, J.A., Meagher, J., Hsie, E.-Y., Edgerton, E., Shaw, S., Trainer, M., 2012. A volatility basis set model for summertime secondary organic aerosols over the eastern United States in 2006. Journal of Geophysical Research 117, 1–19. https://doi.org/10.1029/2011JD016831.

Akbari, H., Bell, R., Brazel, T., Cole, D., Estes, M., Heisler, G., Hitchcock, D., Lewis, M., McPherson, G., Oke, T., Parker, D., Perrin, A., Rosenthal, J., Sailor, D., Samenow, J., Taha, H., Voogt, J., Winner, D., Wolf, K., Zalph, B., 2008. Urban heat island basics. In: Hogan, K., Rosenberg, J., Denny, A. (Eds.), Reducing Urban Heat Islands: Compendium of Strategies. United States Environmental Protection Agency, U.S., pp. 1–22

Akbari, H., Davis, S., Dorsano, S., Huang, J., Winnett, S., 1992. Cooling Our Communities: a Guidebook on Tree Planting and Light Colored Surfacing. U.S. Environmental Protection Agency, Office of Policy Analysis, Climate Change Division, Berkeley.

Athanasopoulou, E., Vogel, H., Vogel, B., Tsimpidi, A.P., Pandis, S.N., Knote, C., Fountoukis, C., 2013. Modeling the meteorological and chemical effects of secondary organic aerosols during an EUCAARI campaign. Atmospheric Chemistry and Physics 13, 625–645. https://doi.org/10.5194/acp-13-625-2013.

Banan, N., Latif, M.T., Juneng, L., Ahamad, F., 2013. Characteristics of surface ozone concentrations at stations with different backgrounds in Malaysia Peninsula. Aerosol Air Quality Research 13, 1090–1106. https://doi.org/10.4209/aaqr.2012.09.0259.

Bell, M.L., Mcdermott, A., Zeger, S.L., Samet, J.M., Dominici, F., 2004. Ozone and short-term mortality in 95 US urban communities, 1987-2000. Journal of the American Medical Association 292, 2372–2378. https://doi.org/10.1001/jama.292.19.2372.

Bhatt, B.C., Sobolowski, S., Higuchi, A., 2016. Simulation of diurnal rainfall variability over the maritime continent with a high-resolution regional climate model. Journal of Meteorological Society of Japan 94A, 89–103. https://doi.org/10.2151/jmsj.2015-052.

Chen, F., Zhang, Y., 2009. On the coupling strength between the land surface and the atmosphere: from viewpoint of surface exchange coefficients. Geophysical Research Letters 36, 1–5. https://doi.org/10.1029/2009GL037980.

Civerolo, K., Hogrefe, C., Lynn, B., Rosenthal, J., Ku, J.-Y., Solecki, W., Cox, J., Small, C., Rosenzweig, C., Goldberg, R., Knowlton, K., Kinney, P., 2007. Estimating the effects of increased urbanization on surface meteorology and ozone concentrations in the New York City metropolitan region. Atmospheric Environment 41, 1803–1818. https://doi.org/10.1016/j.atmosenv.2006.10.076.

Civerolo, K.L., Sistla, G., Rao, S.T., Nowak, D.J., 2000. The effects of land use in meteorological modeling: implications for assessment of future air quality scenarios. Atmospheric Environment 34, 1615–1621.

Clappa, L.J., Jenkin, M.E., 2001. Analysis of the relationship between ambient levels of O_3, NO_2 and NO as a function of NO_x in the UK. Atmospheric Environment 35, 6391–6405.

Department of Environment, 2013. New Malaysia Ambient Air Quality Standard. Petaling Jaya.

Department of Statistics, 2011. Population distribution by local authority areas and mukims, 2010: tables of local authority areas in Selangor. Department of Statistic Malaysia: Population and Housing Census of Malaysia, Putrajaya, pp. 181–201.

Dee, D.P., Uppala, S.M., Simmons, A.J., Berrisford, P., Poli, P., Kobayashi, S., Andrae, U., Balmaseda, M.A., Balsamo, G., Bauer, P., Beschtold, P., Beljaars, A.C.M., van deBerg, L., Bidlot, J., Bormann, N., Delsol, C., Dragani, R., Fuentes, M., Geer, A.J., Haimberger, L., Healy, S.B., Hersbach, H., Hólm, E.V., Isaksen, L., Kållberg, P., Köhler, M., Matricardi, M., Mcnally, A.P., Monge-Sanz, B.M., Morcrette, J.J., Park, B.K., Peubey, C., deRosnay, P., Tavolato, C., Thépaut, J.N., Vitart, F., 2011. The ERA-Interim reanalysis: configuration and performance of the data assimilation system. Quarterly Journal of the Royal Meteorological Society 137, 553–597.

Dimoudi, A., Nikolopoulou, M., 2003. Vegetation in the urban environment: microclimatic analysis and benefits. Energy and Buildings 35, 69–76.

Duenas, C., Fernández, M.C., Canete, S., Carretero, J., Liger, E., 2002. Assessment of ozone variations and meteorological effects in an urban area in the Mediterranean coast. The Science of the Total Environment 299, 97–113. https://doi.org/10.1016/S0048-9697(02)00251-6.

Emery, C., Tai, E., Yarwood, G., 2001. Enhanced Meteorological Modeling and Performance Evaluation for Two Texas Ozone Episodes. Environ International Corporation, California, US.

Emmons, L.K., Walters, S., Hess, P.G., Lamarque, J.-F., Pfister, G.G., Fillmore, D., Granier, C., Guenther, A., Kinnison, D., Laepple, T., Orlando, J., Tie, X., Tyndall, G., Wiedinmyer, C., Baughcum, S.L., Kloster, S., 2010. Description and evaluation of the model for ozone and related chemical tracers, version 4 (MOZART-4). Geoscientific Model Development 3, 43–67.

Fallmann, J., Forkel, R., Emeis, S., 2016. Secondary effects of urban heat island mitigation measures on air quality. Atmospheric Environment 125, 199–211. https://doi.org/10.1016/j.atmosenv.2015.10.094.

Foley, J.A., DeFries, R., Asner, G.P., Barford, C., Bonan, G., Carpenter, S.R., Stuart Chapin, F., Coe, M.T., Daily, G.C., Gibbs, H.K., Helkowski, J.H., Holloway, T., Howard, E.A., Kucharik, C.J., Monfreda, C., Patz, J.A., Colin Prentice, I., Ramankutty, N., Snyder, P.K., 2005. Global consequences of land use. Science 309, 570–574.

Freitas, S.R., Longo, K.M., Alonso, M.F., Pirre, M., Marecal, V., Grell, G., Stockler, R., Mello, R.F., Sánchez Gácita, M., 2011. PREP-CHEM-SRC – 1.0: a preprocessor of trace gas and aerosol emission fields for regional and global atmospheric chemistry models. Geoscientific Model Development 4, 419–433. https://doi.org/10.5194/gmd-4-419-2011.

Gao, H., Jia, G., 2013. Assessing disagreement and tolerance of misclassification of satellite-derived land cover products used in WRF model applications. Advances in Atmospheric Sciences 30, 125–141. https://doi.org/10.1007/s00376-012-2037-4.

Guenther, A., Karl, T., Harley, P., Wiedinmyer, C., Palmer, P.I., Geron, C., 2006. Estimates of global terrestrial isoprene emissions using MEGAN (Model of Emissions of Gases and Aerosols from Nature). Atmospheric Chemistry and Physics Discussions 6, 107–173.

Grossman-Clarke, S., Liu, Y., Zehnder, J.A., Fast, J.D., 2008. Simulations of the urban planetary boundary layer in an arid metropolitan area. Journal of Applied Meteorology Climatology 47, 752–768. https://doi.org/10.1175/2007JAMC1647.1.

Han, S., Bian, H., Feng, Y., Liu, A., Li, X., Zeng, F., Zhang, X., 2011. Analysis of the relationship between O_3, NO and NO_2 in Tianjin, China. Aerosol Air Quality Research 11, 128–139. https://doi.org/10.4209/aaqr.2010.07.0055.
Janjic, Z.I., 2001. Nonsingular Implementation of the Mellor-yamada Level 2.5 Scheme in the NCEP Meso Model. NOAA/NWS/NCEP Off. Note 437.
Jauregui, E., Godinez, L., Cruz, F., 1992. Aspects of heat-island development in Guadalajara, Mexico. Atmospheric Environment 26B, 391–396.
Jiang, X., Wiedinmyer, C., Chen, F., Yang, Z.L., Lo, J.C.F., 2008. Predicted impacts of climate and land use change on surface ozone in the Houston, Texas area. Journal of Geophysical Research 113, 1–16. https://doi.org/10.1029/2008JD009820.
Kalnay, E., Cai, M., 2003. Impact of urbanization and land-use change on climate. Nature 423, 528–531. https://doi.org/10.1038/nature01675.
Kataoka, K., Matsumoto, F., Ichinose, T., Taniguchi, M., 2009. Urban warming trends in several large Asian cities over the last 100 years. The Science of the Total Environment 407, 3112–3119. https://doi.org/10.1016/j.scitotenv.2008.09.015.
Kavassalis, S.C., Murphy, J.G., 2017. Understanding ozone-meteorology correlations: a role for dry deposition. Geophysical Research Letters 44, 2922–2931. https://doi.org/10.1002/2016GL071791.
Kikuchi, K., Wang, B., 2008. Diurnal precipitation regimes in the global tropics. Journal of Climate 21, 2680–2696. https://doi.org/10.1175/2007JCLI2051.1.
Lacour, S.A., deMonte, M., Diot, P., Brocca, J., Veron, N., Colin, P., Leblond, V., 2006. Relationship between ozone and temperature during the 2003 heat wave in France: consequences for health data analysis. BMC Public Health 6. https://doi.org/10.1186/1471-2458-6-261.
Lai, L.-W., Cheng, W.-L., 2009. Air quality influenced by urban heat island coupled with synoptic weather patterns. The Science of the Total Environment 407, 2724–2733. https://doi.org/10.1016/j.scitotenv.2008.12.002.
Latif, M.T., Lim, S.H., Juneng, L., 2012. Variations of surface ozone concentration across the Klang Valley, Malaysia. Atmospheric Environment 61, 434–445. https://doi.org/10.1016/j.atmosenv.2012.07.062.
Lee, T.-W., Choi, H.S., Lee, J., 2014. Generalized scaling of urban heat island effect and its applications for energy consumption and renewable energy. Advanced Meteorology 2014, 1–5. https://doi.org/10.1155/2014/948306.
Li, J., Georgescu, M., Hyde, P., Mahalov, A., Moustaoui, M., 2014. Achieving accurate simulations of urban impacts on ozone at high resolution. Environmental Research Letters 9, 1–11. https://doi.org/10.1088/1748-9326/9/11/114019.
Li, X.X., Koh, T.Y., Entekhabi, D., Roth, M., Panda, J., Norford, L.K., 2013. A multi-resolution ensemble study of a tropical urban environment and its interactions with the background regional atmosphere. Journal of Geophysical Research Atmosphere 118, 9804–9818. https://doi.org/10.1002/jgrd.50795.
Mahmood, R., Pielka, R.A.S., Hubbard, K.G., Niyogi, D., Bonan, G., More, 2010. Impacts of land use/land cover change on climate and future research priorities. Bulletin of the American Meteorological Society 91, 37–46. https://doi.org/10.1175/2009BAMS2769.1.
Martilli, A., Clappier, A., Rotach, M.W., 2002. An urban surface exchange parameterisation for mesoscale models. Boundary Layer Meteorology 104, 261–304.
Morris, K.I., 2016. Computational Study of Klang Valley's Urban Climatology, and Urbanisation of Putrajaya City, Malaysia. Nottingham EPrints. University of Nottingham.
Oke, T.R., 1976. The distinction between canopy and boundary - layer urban heat islands. Atmosphere (Basel) 14, 37–41. https://doi.org/10.1080/00046973.1976.9648422.
Oke, T.R., 1973. City size and the urban heat island. Atmospheric Environment 7, 769–779.
Oke, T.R., Maxwell, G.B., 1975. Urban heat island dynamics in Montreal and Vancouver. Atmospheric Environment 9, 191–200.
Ono, R., Nakagawa, Y., Tokumitsu, Y., Matsumoto, H., Oda, T., 2014. Effect of humidity on the production of ozone and other radicals by low-pressure mercury lamps. Journal of Photochemistry and Photobiology A Chemistry 274, 13–19. https://doi.org/10.1016/j.jphotochem.2013.09.012.
Ooi, M.C.G., Chan, A., Ashfold, M.J., Morris, K.I., Oozeer, M.Y., Salleh, S.A., 2017. Numerical study on effect of urban heating on local climate during calm intermonsoon period in greater Kuala Lumpur, Malaysia. Urban Climate 20, 228–250. https://doi.org/10.1016/j.uclim.2017.04.010.
Ooka, R., Khiem, M., Hayami, H., Yoshikado, H., Huang, H., Kawamoto, Y., 2011. Influence of meteorological conditions on summer ozone levels in the central Kanto area of Japan. Procedia Environmental Science 4, 138–150. https://doi.org/10.1016/j.proenv.2011.03.017.
Pielke, R.A., Pitman, A., Niyogi, D., Mahmood, R., McAlpine, C., Hossain, F., Goldewijk, K.K., Nair, U., Betts, R., Fall, S., Reichstein, M., Kabat, P., deNoblet, N., 2011. Land use/land cover changes and climate: modeling analysis and observational evidence. Wiley Interdiscipline Review of Climate Change 2, 828–850. https://doi.org/10.1002/wcc.144.
Pudasainee, D., Sapkota, B., Shrestha, M.L., Kaga, A., Kondo, A., Inoue, Y., 2006. Ground level ozone concentrations and its association with NO_x and meteorological parameters in Kathmandu valley. Nepalese Atmospheric Environment 40, 8081–8087. https://doi.org/10.1016/j.atmosenv.2006.07.011.
Pusede, S.E., Steiner, A.L., Cohen, R.C., 2015. Temperature and recent trends in the chemistry of continental surface ozone. Chemical Reviews 115, 3898–3918. https://doi.org/10.1021/cr5006815.
Romero, H., Ihl, M., Rivera, A., Zalazar, P., Azocar, P., 1999. Rapid urban growth, land-use changes and air pollution in Santiago. Chilean Atmospheric Environment 33, 4039–4047.
Roth, M., 2007. Review of urban climate research in (sub)tropical regions. International Journal of Climatology 27, 1859–1873. https://doi.org/10.1002/joc.
Ryu, Y.-H., Baik, J.-J., Kwak, K.-H., Kim, S., Moon, N., 2013a. Impacts of urban land-surface forcing on ozone air quality in the Seoul metropolitan area. Atmospheric Chemistry and Physics 13, 2177–2194. https://doi.org/10.5194/acp-13-2177-2013.
Ryu, Y.-H., Baik, J.-J., Lee, S.-H., 2013b. Effects of anthropogenic heat on ozone air quality in a megacity. Atmospheric Environment 80, 20–30. https://doi.org/10.1016/j.atmosenv.2013.07.053.
Santamouris, M., 2015. Analyzing the heat island magnitude and characteristics in one hundred Asian and Australian cities and regions. The Science of the Total Environment 512–513, 582–598. https://doi.org/10.1016/j.scitotenv.2015.01.060.
Schultz, M., Rast, S., van het Bolscher, M., Pulles, T., Brand, R., Pereira, J., Mota, B., Spessa, A., Dalsoren, S., van Nojie, T., Szopa, S., 2007. RETRO Deliverable D1–6, Report on Emissions. 5th EU framework programme, Hamburg.
Sertel, E., Robock, A., Ormeci, C., 2009. Impacts of land cover data quality on regional climate. International Journal of Climatology 1–12. https://doi.org/10.1002/joc.
Sillman, S., 1999. The relation between ozone, NOx and hydrocarbons in urban and polluted rural environments. Atmospheric Environment 33, 1821–1845.
Silva, S.J., Heald, C.L., Geddes, J.A., Austin, K.G., Kasibhatla, P.S., Marlier, M.E., 2016. Impacts of current and projected oil palm plantation expansion on air quality over Southeast Asia. Atmospheric Chemistry and Physics 16, 10621–10635. https://doi.org/10.5194/acp-16-10621-2016.
Sow, K.S., Juneng, L., Tangang, F.T., Hussin, A.G., Mahmud, M., 2011. Numerical simulation of a severe late afternoon thunderstorm over Peninsular Malaysia. Atmospheric Research 99, 248–262. https://doi.org/10.1016/j.atmosres.2010.10.014.
Stewart, I., Oke, T.R., 2012. Local climate zones for urban temperature studies. Bulletin of the American Meteorological Society 93, 1879–1900. https://doi.org/10.1175/BAMS-D-11-00019.1.
Stockwell, W.R., Middleton, P., Chang, J.S., Yang, X., 1990. The second generation regional acid deposition model chemical mechanism for regional air quality modeling. Journal of Geophysical Research 95, 16343–16367.
Streets, D.G., Bond, T.C., Carmichael, G.R., Fernandes, S.D., Fu, Q., He, D., Klimont, Z., Nelson, S.M., Tsai, N.Y., Wang, M.Q., Woo, J.-H., Yarber, K.F., 2003. An inventory of gaseous and primary aerosol emissions in Asia in the year 2000. Journal of Geophysical Research 108 (8809). https://doi.org/10.1029/2002JD003093.
Tan, K.C., Lim, H.S., Mat Jafri, M.Z., 2014. Multiple regression analysis in modeling of columnar ozone in Peninsular Malaysia. Environmental Science and Pollution Research International 21, 7567–7577. https://doi.org/10.1007/s11356-014-2697-y.
Tangang, F.T., 2001. Low frequency and quasi-biennial oscillations in the Malaysian precipitation anomaly. International Journal of Climatology 21, 1199–1210. https://doi.org/10.1002/joc.676.
Thompson, W.T., Holt, T., Pullen, J., 2007. Investigation of a sea breeze front in an urban environment. Quarterly Journal of the Royal Meteorological Society 133, 579–594. https://doi.org/10.1002/qj.52.
Tie, X., Brasseur, G., Ying, Z., 2010. Impact of model resolution on chemical ozone formation in Mexico City: application of the WRF-Chem model. Atmospheric Chemistry and Physics 10, 8983–8995. https://doi.org/10.5194/acp-10-8983-2010.
United Nations, 2014. World Urbanization Prospects: the 2014 Revision. Highlights, New York.
Wakamatsu, S., Uno, I., Ohara, T., Schere, K.L., 1999. A study of the relationship between photochemical ozone and its precursor emissions of nitrogen oxides and hydrocarbons in Tokyo and surrounding areas. Atmospheric Environment 33, 3097–3108. https://doi.org/10.1016/S1352-2310(97)00493-7.
Wang, H., Fu, L., Chen, J., 2010. Developing a high-resolution vehicular emission inventory by integrating an emission model and a Traffic model: Part 2—a case study in Beijing. Journal of the Air & Waste Management Association 60, 1471–1475. https://doi.org/10.3155/1047-3289.60.12.1471.
Wang, X.M., Lin, W.S., Yang, L.M., Deng, R.R., Lin, H., 2007. A numerical study of influences of urban land-use change on ozone distribution over the Pearl River Delta region, China. Tellus 59B, 633–641. https://doi.org/10.1111/j.1600-0889.2007.00271.x.
Willmott, C.J., Matsuura, K., 2005. Advantages of the mean absolute error (MAE) over the root mean square error (RMSE) in assessing average model performance. Climate Research 30, 79–82.
Yu, M., Carmichael, G.R., Zhu, T., Cheng, Y., 2012. Sensitivity of predicted pollutant levels to urbanization in China. Atmospheric Environment 60, 544–554. https://doi.org/10.1016/j.atmosenv.2012.06.075.
Yu, S., Eder, B., Dennis, R., Chu, S.-H., Schwartz, S.E., 2006. New unbiased symmetric metrics for evaluation of air quality models. Atmospheric Science Letters 7, 26–34. https://doi.org/10.1002/asl.125.
Zhang, N., Zhu, L., Zhu, Y., 2011. Urban heat island and boundary layer structures under hot weather synoptic conditions: a case study of Suzhou City, China. Advances in Atmospheric Sciences 28, 855–865. https://doi.org/10.1007/s00376-010-0040-1.
Zhang, Q., Streets, D.G., Carmichael, G.R., He, K.B., Huo, H., Kannari, A., Klimont, Z., Park, I.S., Reddy, S., 2009. Asian emissions in 2006 for the NASA INTEX-B mission. Atmospheric Chemistry and Physics 9, 5131–5153.
Zhao, L., Lee, X., Smith, R.B., Oleson, K., 2014. Strong contributions of local background climate to urban heat islands. Nature 511, 216–219. https://doi.org/10.1038/nature13462.
Zhong, S., Yang, X.Q., 2015. Ensemble simulations of the urban effect on a summer rainfall event in the Great Beijing Metropolitan Area. Atmospheric Research 153, 318–334. https://doi.org/10.1016/j.atmosres.2014.09.005.